JOURNAL OF MATERIALS SCIENCE 27 (1992) 3624–3636

Investigation by scanning electron microscope of the effect of geometry and loading mode on blunting of copper sheets

P. S. THEOCARIS, V. N. KYTOPOULOS
Department of Engineering Sciences, The National Technical University, PO Box 77230, 17510 Athens, Greece

Ductile blunting and fracture under conditions of plane stress in metals are described by two main phases: static crack growth, and slow crack propagation. In the first phase the crack tip is deformed in an elastic–plastic mode, the main characteristics of which are the formation of the plastic enclave around the crack tip, and the evolution of blunting. In the second phase the crack propagates through expansion and coalescence of microvoids and microdefects developed at the vicinity of and in front of the crack tip. Ductile blunting under plane-stress conditions in metallic plates was studied, and the influence of the geometry and the mode of loading specimens was defined. This was achieved by interrelating the amount of crack opening displacement at its tip, and its comparable effect of the crack tip advance displacement. The experimental study was executed in a scanning electron microscope with thin specimens under dominating plane-stress conditions. The mechanism of development of ductile blunting up to the point of initiation of slow crack propagation was interrelated with these characteristic quantities.

1. Introduction

Attempts to match the crack-tip region plasticity with blunting involve post net-section yielding fracture behaviour in laboratory specimens of reduced size. However, for a tough material, fracture may occur in such small laboratory specimens at loads beyond the general yielding. On the other hand, large structural members made of the same tough material containing a crack may fracture at a low stress level in a brittle manner. The lack of information on the plastic deformation near a crack tip prevents the correlation of the ductile fracture behaviour of small laboratory specimens of a tough material to the brittle fracture behaviour of a large structural component made of the same material.

Wells [1] suggested the crack-tip opening displacement (CTOD) as a reliable parameter which might be used to describe the plastic behaviour of a tough material when crack propagation occurs after extensive yielding. The great importance of CTOD lies in the fact that it may be considered as a measure of the material toughness of a ductile material, and even for small thicknesses of specimens is better than the stress intensity factor K or the J-integral concepts, as it affords less stringent limits of applications related to their validity for plane-strain conditions [2].

Numerous encouraging investigations in different countries have followed the suggestion of Wells, which has found widespread application to welded structural steels [3]. Nevertheless, doubts are still expressed regarding both the physical occurrence and the definition of CTOD [4, 5]. This is why various experimental methods have been devised for the measurement of CTOD in plane strain, including the optical method [6, 7]; the metallographical method [8, 9]; the fractographical [4, 10]; the stereofractographical [11, 12]; the acoustical [13]; and the geometrical–graphical method [14–16]. The major disadvantage of all these methods consists in the fact that they are indirect, cumbersome, time-consuming methods, based on different theoretical assumptions [12].

For a certain plate thickness the critical CTOD expresses the strength of the material to ductile fracture. Thus equal practical interest presents an accurate measurement of the critical CTOD of very thin specimens in dominating plane-stress conditions where a gross yielding always happens before fracture conditions, which does not appear always in plane-strain. In this way the difficulties in explaining the large scatter of results in the measurement of the critical CTOD are avoided, as the stretched zones are measured in thick and thin specimens [11], as well as the difficulty in measuring the critical CTOD by the doubtful definition of the localization of crack initiation by the existing crack-monitoring methods [13, 16, 17] because of the appearance of the tunnelling effect in thick specimens.

Because of all these inconveniences, our knowledge concerning the morphological evolution of the phenomenon of blunting of a sharp crack tip in plane stress, and the factors which influence this phenomenon is limited. Recent SEM experiments in polycarbonate [18–21] under conditions of plane stress indicated the necessity of further studies by this

0022–2461

powerful method in order to examine some of these questions. A similar study in metals and polycrystalline strain-hardening materials is of interest, where because of the multiple slip systems of plastic flow [22] developed in these materials, certain theoretical features in the morphology of blunting appear [23].

Concerning the *in situ* SEM experiments, studies have been sparse and of a general character [24]. An experimental SEM study concerning the morphological evolution of blunting is in general restricted to study of the surface of the specimen, which is always under conditions of plane stress. Thus the whole problem is mainly focused on the study of surface-blunting phenomenon, and therefore on the surface crack-tip opening displacement (S-CTOD).

However, in studying thin plates the surface blunting is modified to an approximate through the thickness or average blunting. In this way we avoid all the difficulties related to thick specimens. In addition, the knowledge of the crack-tip surface phenomena for thin specimens is by itself important for studying the mechanics of fracture. Thus the evaluation of the critical S-CTOD is of great importance for the study of the various fracture criteria [25], as well as for the study of the various treatments of the materials where intense residual surface-stress effects are evinced [26].

2. Experimental procedure

The material used in the SEM tests was of copper sheets of a high residual phosphorous copper containing 0.1% P(HPC) cold rolled and annealed at 600 °C, commercially pure with a purity 99.8% copper. The copper sheets had the following typical directional properties: a ductility parallel to the rolling direction (RD) equal to 46%, and ductilities along 45° and 90° to RD were 53 and 55%, respectively.

The specimens prepared from the copper sheets were of the single-edge cracked tension type (SECT) with different crack geometries defined by the ratio (α/w) of the initial crack length to the width of specimens. The initial sharp crack tip was prepared with high precaution as an artificial crack with the help of a jeweller's fine saw. With an elaborate technique of successive saw cutting we succeeded in creating sufficiently sharp crack tips to avoid the procedure of creating sharp crack tips through fatigue. Fatigue crack extension always results in the creation of a plastic enclave around the crack flanks which, during recrystallization softening, develops a grain distribution continuously increasing in size from the crack tip outwards. This alters the texture of the material and progressively influences the yield strength of the material [27], thus affecting its mode of blunting [28].

However, the shape and form achieved by careful sawing of the plates ascertained a satisfactory sharpness, so that the artificial cracks may be considered as actual sharp cracks. A series of double-edge cracked thin specimens with skew parallel cracks (DECT) were also tested in order to study further the typical mixed-mode loadings under conditions of plane stress.

Finally, starting from an initial plate thickness $d = 1.5$ mm, and by chemical etching with the help of a convenient solution of HNO_3, we further reduced the thicknesses of the cracked plates to the desired thicknesses. In cases where, after etching, it was necessary to dispose an accurately uniform thickness, this was achieved by mechanical polishing through the use of 600 grit SiC polish.

3. Results

3.1 Morphological evolution of blunting under mode-I loading

With the prepared copper specimens we first undertook an *in situ* SEM study of the morphological evolution of blunting of an initially sharp crack tip under conditions of dominating plane stress. Several theoretical and experimental studies on the form of blunting under conditions of dominating plane-strain have recently been presented [29–31]. However, the phenomenon of blunting under plane stress appeared only recently, dealing with the blunting modes of thin plates of polycarbonate (Lexan) [18–21]. As blunting modes in polymers are completely different from the blunting in polycrystalline materials, it was the purpose of this work to undertake an experimental study in thin copper plates, in order to reveal the similarities and differences between the modes of blunting of the two types of materials.

Fig. 1 presents a relatively round blunting developed during the first steps of loading of a thick specimen of $d = 1.5$ mm. Because of the large depth of focus of the scanning electron microscope (150 μm for an enlargement $\times 1000$), we can observe simultaneously the form of blunting dominating along the thickness of the specimen up to its rear face. It can be observed that the blunting of the rear face is not exactly circular, as is the blunting of the front face, but it is significantly flattened.

Fig. 2 presents the evolution of blunting of the front face of a thinner plate ($d = 1.0$ mm, $\times$ 500). A typical round initial blunting appears also in Fig. 2a, which tends to develop an outflattening in Fig. 2b and afterwards the procedure of initiation of a slow crack propagation takes place, indicated in Fig. 2c and d.

In some specimens we intentionally left various marks on the surface of the specimens which were used afterwards as points of reference, in order to estimate the quantitative evolution of blunting. Thus, if one takes as a point of reference the white dot A in Fig. 2a, it can be seen from the relative position of this dot in the subsequent photographs that, besides the increase of the CTOD in Fig. 2 b–d, there is also an extension and propagation of the crack tip inside the specimen corresponding to a crack-tip advance displacement (CTAD) [32]. By comparing Fig. 2c and d we can see at once that the CTAD continues to increase more rapidly in the phase of the slow crack propagation.

The same results can be derived from Fig. 3a and b with the difference that the final form of blunting in this test is different from Fig. 2b. Thus, in Fig. 3b an intense form of a tooth-root appears much more pronounced than in Fig. 2b.

Fig. 3 presents the initial steps of evolution of

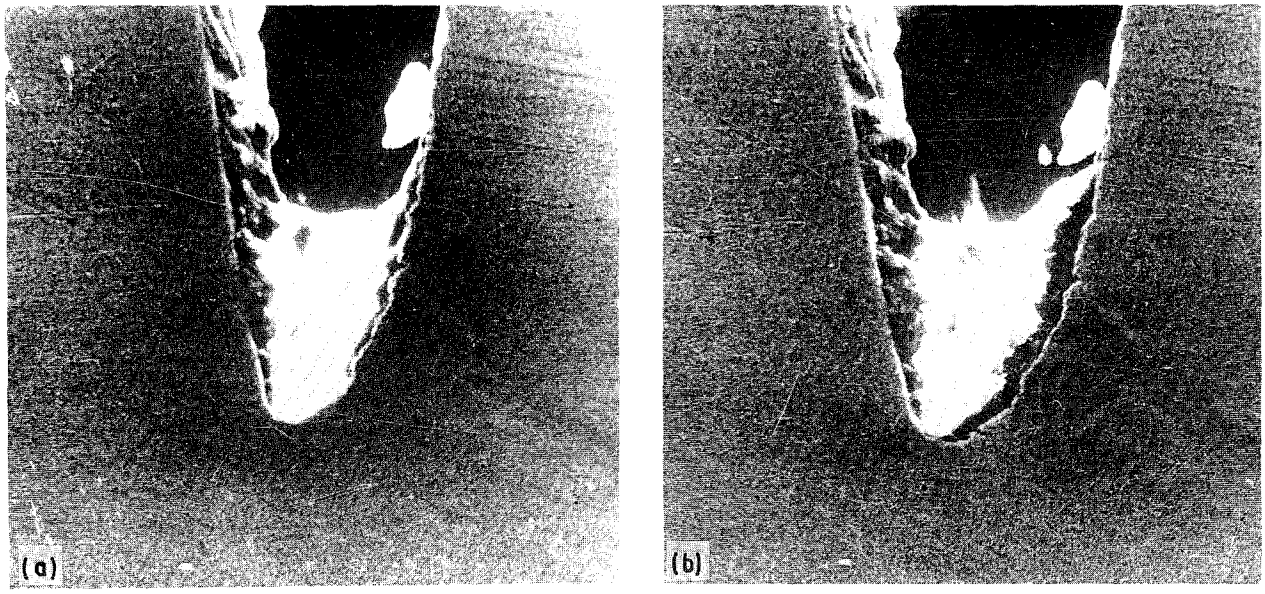

Figure 1 Scanning electron micrographs for cracked copper plates under mode-I deformation, indicating the round type of blunting ($d = 1.5$ mm).

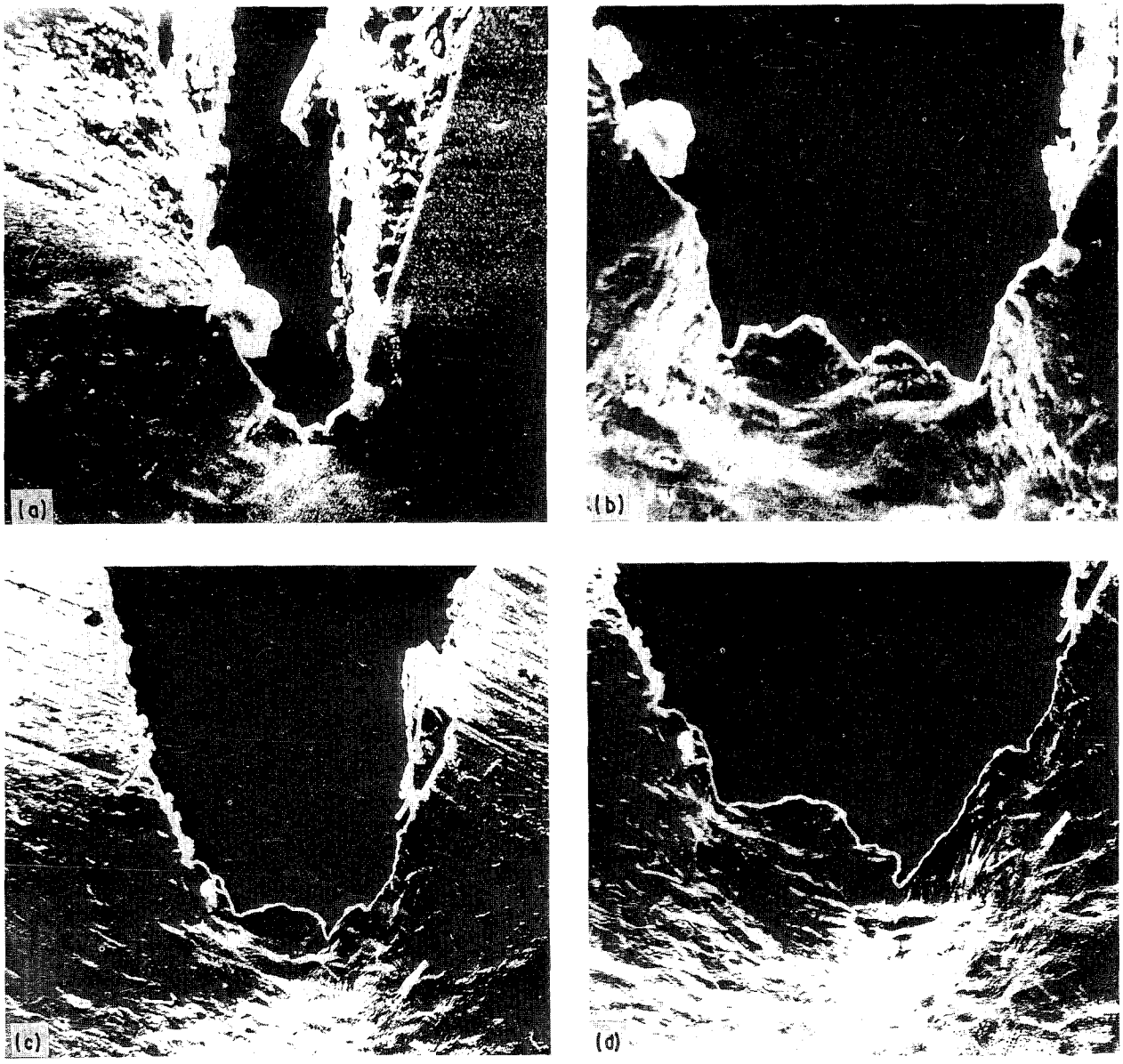

Figure 2 Scanning electron micrographs for cracked copper plates under mode-I deformation, presenting the outflattened type of blunting with several roots ($d = 1.0$ mm).

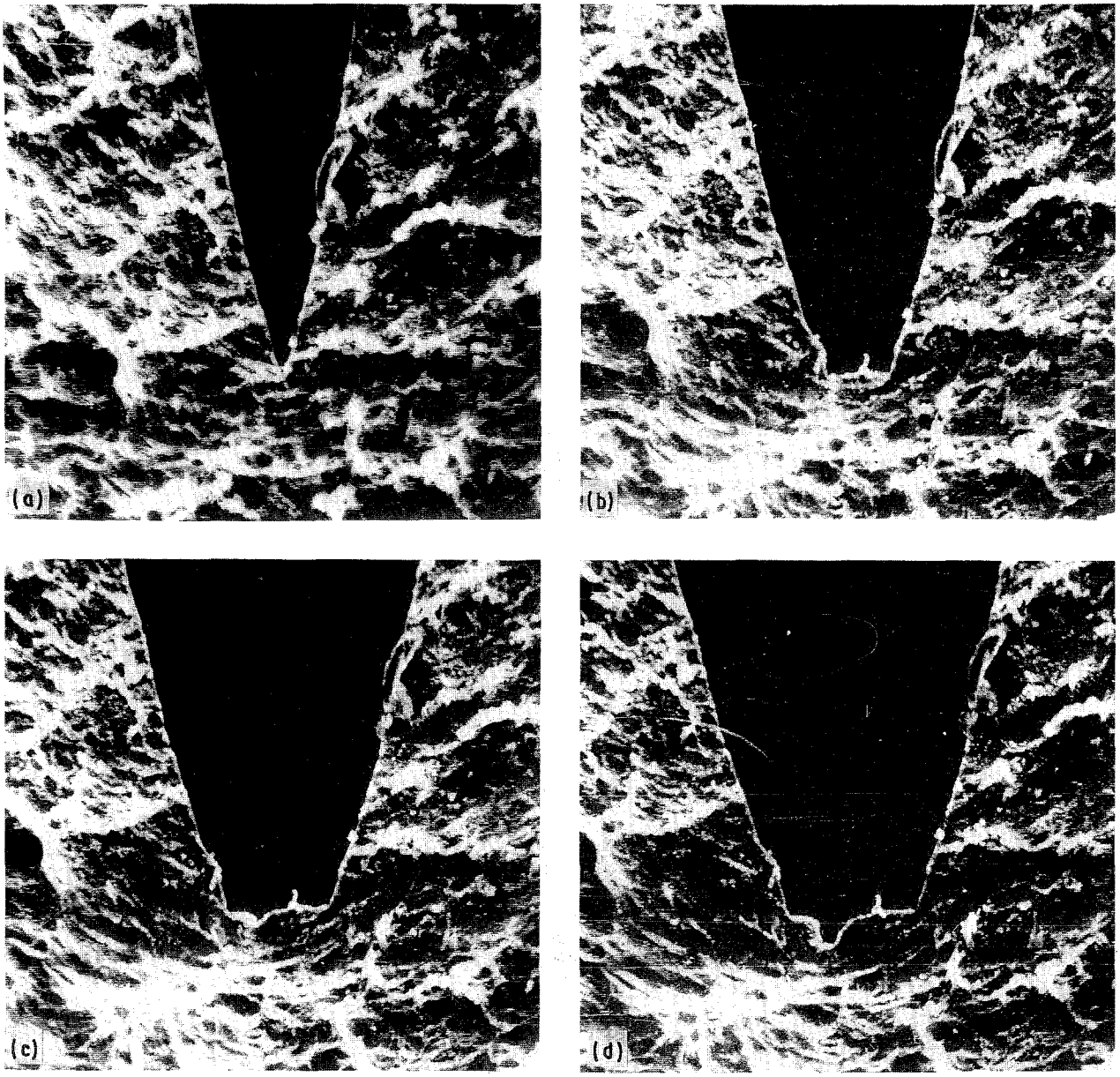

Figure 3 Scanning electron micrographs for cracked copper plates under mode-I deformation, presenting the outflattened type of blunting with several roots for very thin plates ($d = 0.2$ mm).

blunting up to the point of initiation of slow crack propagation for a very thin specimen ($d = 0.20$ mm, $\times$ 500) where strong conditions of plane stress dominate at the crack tip. In Fig. 3b, as well as in Fig. 2b, an intense bright field also develops, creating an enclave around the out-flattening front of the blunted crack, which is due to a plastic flow field completely covering the CTAD along the length of the developed flanks of the blunting.

Whereas Figs 2 and 3 present the evolution of blunting in cracks subjected to a mode-I loading, Fig. 4 presents successive steps of loading and development of blunting for a crack under a mixed mode of loading. Indeed, the crack is an oblique one whose symmetry axis subtends an angle $\beta = 70°$ with the loading axis. The thickness of the cracked plate is $d = 0.80$ mm $\times$ 500 and the blunting patterns resemble those for a plane-stress loading.

From the extensive experimental evidence with ductile blunting under plane-stress conditions, as exemplified by Figs 2 and 3, the general trend of evolution of this phenomenon can be described as follows.

(i) The size of the two external roots developed along the front of the blunted crack close to its flanks influences the number and size of the vertices appearing along this front. The larger the size of the extreme roots, the larger the number of vertices and their sizes.
(ii) The outflattening of the crack front also creates the development of the bright field in front of the blunted crack, which becomes more intense at the time of initiation of the slow crack propagation.
(iii) In between the front of the blunted crack and the bright field, there always exists a thin strand of lower strains, which is always darker than the plastic bright field. This zone corresponds to the elastic enclave incorporated inside the plastic zone, which has been studied by Rice

and Johnson for plain-strain conditions and mode-I deformation [30], and by Theocaris for plane stress conditions and either mode-I or mixed-modes deformation [20]. It was shown that this zone of lower straining is much less wide for plane stress than for plane strain [20].

(iv) For stronger conditions of plane stress, that is for thinner plates, the elastic enclave becomes thinner; the front outflattening of the crack becomes smoother with a limited number of roots; and the critical CTOD is considerably reduced. Thus, as the thickness of the plate is diminishing the CTOD is reduced and not only the internal roots and microindentations disappear, but also the extreme pronounced roots.

(v) This phenomenon results in a delay of the initiation of slow crack propagation. This suspense of the initiation of the phase of crack propagation results in an increase of the strain energy stored at the crack tip and a subsequent development of a rapid brittle fracture.

3.2. Blunting under mixed-mode loading

Fig. 4 presents the ductile blunting under conditions of mixed-mode loading. An oblique crack whose axis initially subtends an angle $\beta = 65°$ with the loading axis of the plate is subjected to simple tension. The thickness of the plate is equal to $d = 0.8$ mm. Therefore, plane-stress conditions of loading dominate. Fig. 4a indicates the initiation of ductile blunting where the crack develops a round front. Now the round front is asymmetrical in relation to the symmetry axis of the crack. At the same stage, an extended bright field develops along the whole convex flank of the crack, indicating the introduction of plasticity at a limited extent. Along the other flank of the crack, the concave one, a wedge of plastic flow is developed much behind the region of the crack tip. This plastic-flow wedge, however, contains enclaves of elastic deformation in triangular forms. Fig. 4b, c presents the evolution stage of ductile blunting the creation of the outflattened front of the crack containing a series of roots of different penetrations inside the plate, and in Fig. 4c the development of a dominant root at the middle of the outflattening of the crack. This is a clear indication that, while at the initiation of ductile blunting the phenomenon is significantly influenced by the mixed mode of loading, subsequently as the critical CTOD is installed the crack behaves as if it was loaded in mode I. The flat front of the blunted crack is much larger than the respective front for mode-I loading, and this front seems to be in an oblique direction with respect to the crack axis.

Fig. 5 presents the development of ductile blunting for a crack whose axis subtends an angle $\beta = 50°$ with the loading axis of the plate. The thickness of this plate is $d = 0.8$ mm. The parallel striations on the surface of this specimen are created during mechanical polishing of the surface with SiC polish. The parallel striations were initially normal to the direction of loading and

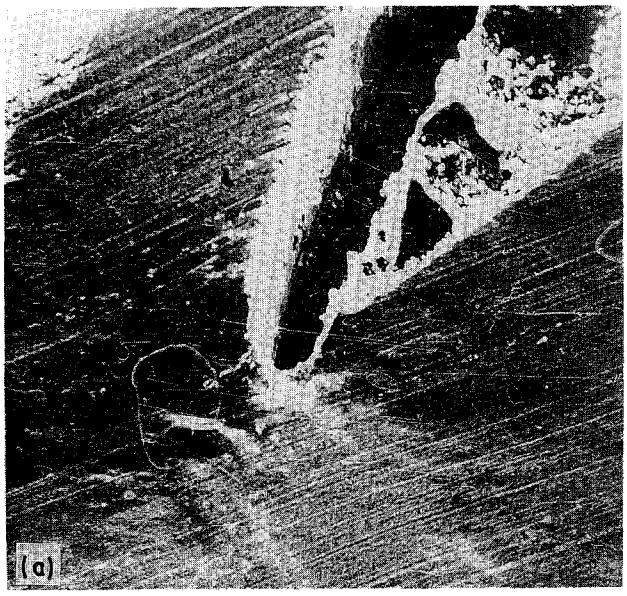

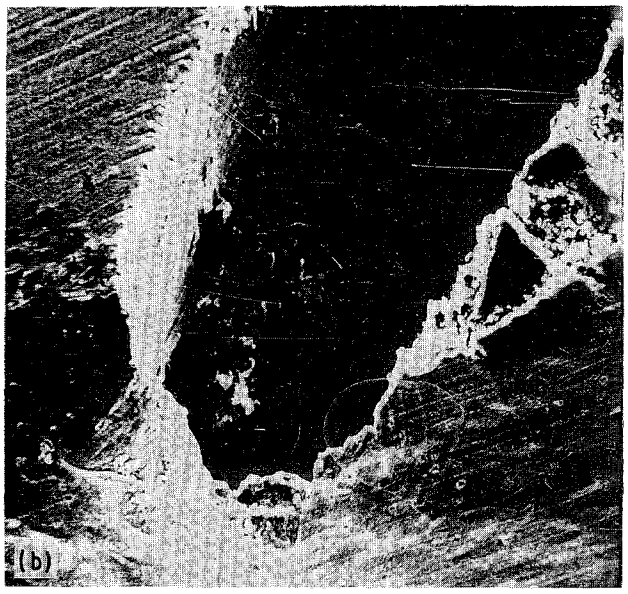

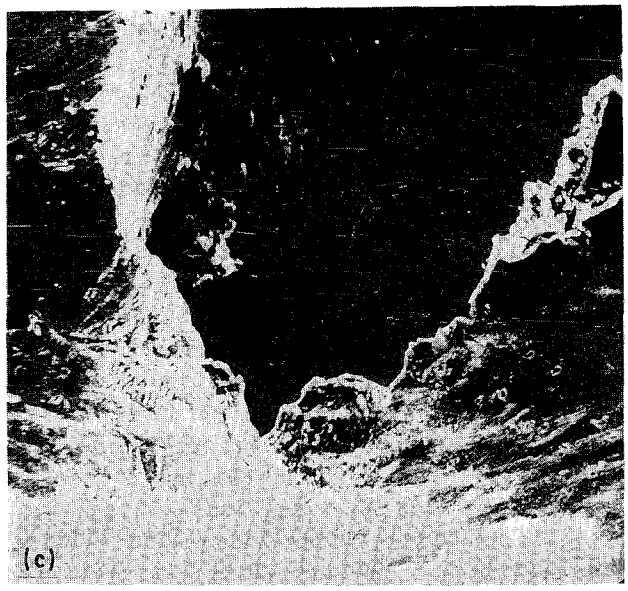

Figure 4 Scanning electron micrographs for cracked copper plates under mixed-mode deformation, presenting the outflattened type of blunting with several roots (single crack, $\beta = 65°$, $d = 0.8$ mm).

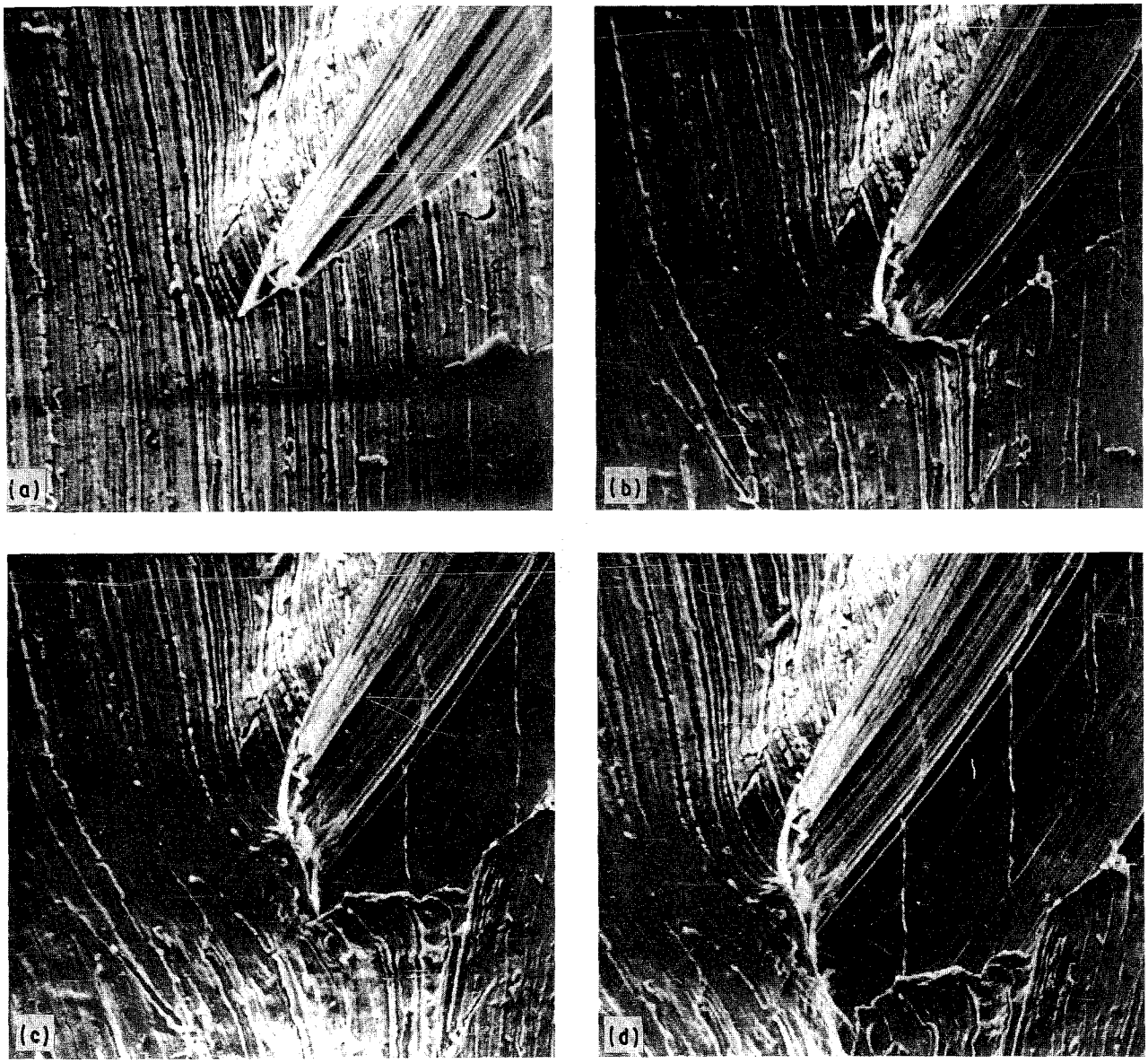

Figure 5 Scanning electron micrographs for cracked copper plates under mixed-mode deformation, presenting the outflattened type of blunting with several roots (single crack, $\beta = 50°$, $d = 0.8$ mm).

thus made it possible to follow the evolution of the deformation yield near the blunted crack tip.

It is clear that a contraction deformation field is developed only along the convex flank of the blunted crack where there is a condensation of striations and a simultaneous distortion, so that a great number of these lines end along this flank (see Fig. 5a, b). As the loading increases and a ductile blunting takes place transforming the sharp tip of the crack into a rounded-off front, the striations follow at the region of high plastic-deformation curves similar to the shape of the blunted crack tip. Furthermore, in the plastic zone developed in front of the crack, which has the shape of a domain limited by logarithmic spirals [20], the striations disappear almost completely because of the large strains developed there. Similar zones of sparse striations develop along the other concave flank of the crack, which also presents an anomalous pattern with a series of indentations. During the development of impending slow crack propagation, where a single and very pronounced kink is developed at the middle of CTOD, the transverse opening of the blunted crack becomes very large and a series of secondary kinks develops along the half of the blunted front neighbouring the concave flank.

Fig. 5c, d presents clearly the initiation and development of these phenomena, and indicate that in front of the out-flattened blunted crack another asymmetrical plastic flow field is developed, indicated by the bright zones. In the same figures it is evident that, besides the development of large CTOD, there is a pronounced CTAD, according to which the crack tip has been advanced significantly, and which is the precursor of the initiation of the slow crack-propagation step.

Moreover, besides the contraction field developed along the convex flank of the crack in Fig. 5, a dilatation field evolves in front of the round blunting of the crack indicated by the rarefaction of the striations there. By examining the plastic enclave in front of the blunted crack tip, indicated by the dark region in a z-modulation arrangement of the scanning microscope, it can be readily proved that this plastic z-deformation is a compressive one, creating a shallow

dimple delineated by logarithmic spirals. A similar study of the blunting phenomena in polycarbonate plates indicated the same phenomenon [20].

Comparing Figs 2b and 4b, it is clear that the same phenomenon of blunting develops in oblique cracks subjected to a mixed mode of loading. Indeed, the same outflattening phenomenon develops for the oblique cracks under plane-stress conditions, as for the cracks in mode I. It may be derived from Figs 2b, 3b and 4b that, as the tooth roots developed in the front of the cracks become deeper, the extreme flank angles of the blunted cracks become larger, and the respective flow fields represented by the bright enclaves in the front vicinity of the crack tips also become larger. Moreover, for the oblique cracks, and in general for cracks under mixed modes of loading, the plastic flow fields are asymmetrical, concentrated mostly along the front concave flank of the crack, and extending as tufts in the forefronts of the crack tips.

Finally in Fig. 6a, b, different forms of ductile blunting are presented in specimens containing two staggered deep edge cracks approaching each other. The cracks at the beginning are skew parallel. This geometry of cracks was selected to be in accordance with remarks of Cotterell *et al.* [33], who suggested that a true mixed-mode ductile fracture can be obtained in thin sheets by the use of such staggered deep-cracked tensile specimens. Thus in Fig. 6a two forms of blunting appear simultaneously, the round form and the outflattened with small roots, whereas in Fig. 6b a smooth outflattened form in the one crack is opposed to the other crack, which presents a typical blunting form with two extreme roots. In both figures the intense bright flow field is apparent formed by two tufts emanating from the roots of either crack tip.

3.3. Evaluation of mode-I ductile blunting

A series of tests was executed with thin copper plates containing either cracks under mode-I loading or cracks under mixed mode. Some additional tests were carried out with specimens containing a pair of skew parallel cracks. The SEM was used for directly measuring the CODs as well as the advancements of the crack tips $\Delta\alpha$. The SEM can focus close to the crack tip, thus allowing an extremely detailed study of this zone. For this purpose small-size specimens were used which did not necessitate any special preparation, and observations and measurements could be executed under either off- or on-load conditions.

Direct measurements of COD and $\Delta\alpha$ were executed at different steps of loading by a direct method described in [18]. High-accuracy measurements of the surface crack-tip opening displacements (S-CTOD) and simultaneously of the surface crack-tip advance displacements (S-CTAD) were executed in order to evaluate the thickness effect on blunting, that is the influence of the lateral constraint factor, and of the crack geometry effect, that is the influence of the in-plane constraint factor, and their influence on S-CTOD and S-CTAD.

Furthermore, based on the simple model introduced in [18] which stipulates that, for ideal plane-strain conditions, the following simple relation is valid [18, 27]

$$2 \times \text{CTAD} \approx \text{CTOD} \qquad (1)$$

we measured discrepancies from the simple Equation 1 under the influence of the factors referred to previously.

If Equation 1 may be used as a formula of reference to measure the discrepancies of the experimental results from the ideal plane-strain state, similarly the different modified Dugdale models may be used as a basis of comparison with the discrepancies measured from the ideal plane-stress state. For this reason, different Dugdale models were eventually used, where either through the use of the extent of the plastic zone

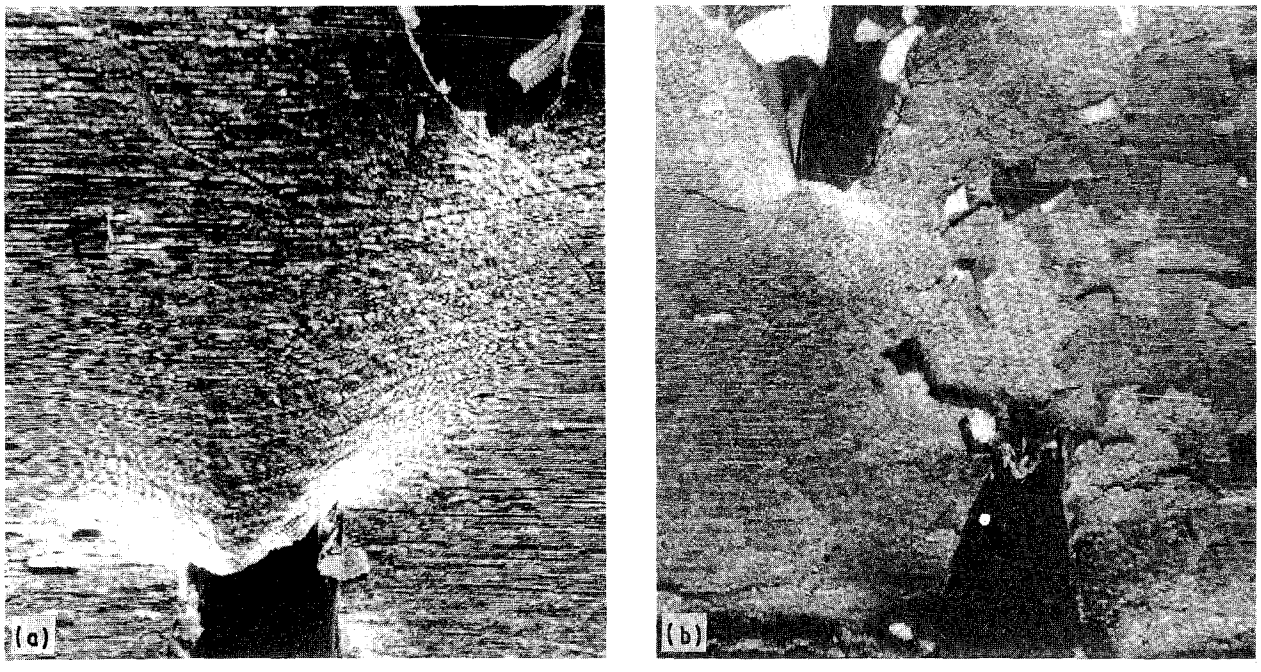

Figure 6 Scanning electron micrographs for copper plates under mixed-mode deformation, containing two staggered edge cracks.

[34–36], or through the measurement of CTOD [37–40], an effort has been made to adapt the results of different tests.

In this paper we have chosen the Isherwood–Williams model [37], as this model expresses CTOD by taking into consideration up to a degree the crack geometry and the strain hardening of the material, which for the case of copper is considerable.

Fig. 7 presents the evolution of CTOD during increasing loading for different thickness of the specimens (d = 0.2, 0.5 and 1.2) and for different ratios of initial crack lengths α to the widths w of the specimens. The continuous line in Fig. 7 represents the theoretical curve for a linear regression of the Isherwood–Williams model. Discrepancies from this line mean discrepancies from the ideal model for plane-stress conditions. By replacing the gross stress σ_∞ at infinity by the net-section stress σ_{net}, we may derive that the in-plane constraint factor, expressed by the ratio α/w, does not significantly influence the results and, furthermore, that thin specimens respond better to the theoretical model than thick specimens, as expected.

The blunting behaviour studied through the evolution of the relationship between S-CTOD and S-CTAD under the influence of the crack geometry is given in Fig. 8 for single-edge and double-edge cracked tension specimens of a thickness d = 1.0 mm and various values of the in-plane constraint factor (α/w). While the initial values all lie in a straight line expressing a relationship approaching Equation 1, for higher values of S-CTAD the slopes of straight lines for DECT and SECT specimens are equal but parallel displaced. These lines, which correspond to loadings approaching the steps of initiation of slow crack propagation, may be expressed by relations of the

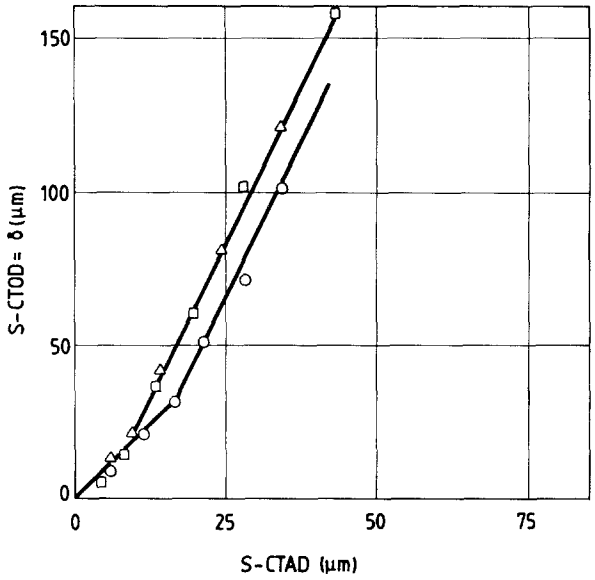

Figure 8 Variation of CTOD against CTAD for a series of specimens of the same thickness d = 1.0 mm and various values of the lateral constraint factor α/w: ○, DECT, 0.4; □, SECT, 0.5; △, SECT, 0.1.

form

$$\lambda(\text{S-CTAD}) \approx \text{S-CTOD} \qquad (2)$$

where the factor λ may be approximated by $\lambda \approx 3.0$ which is in agreement with values given in [21] (whereas for the case of polycarbonate specimens λ was given as 5.5 [21]).

The influence of the thickness d of the specimens, that is of the lateral constraint factor, is presented in Fig. 9 for three different thicknesses (d = 0.2, 0.7 and 1.5 mm). It can be derived from this figure that in

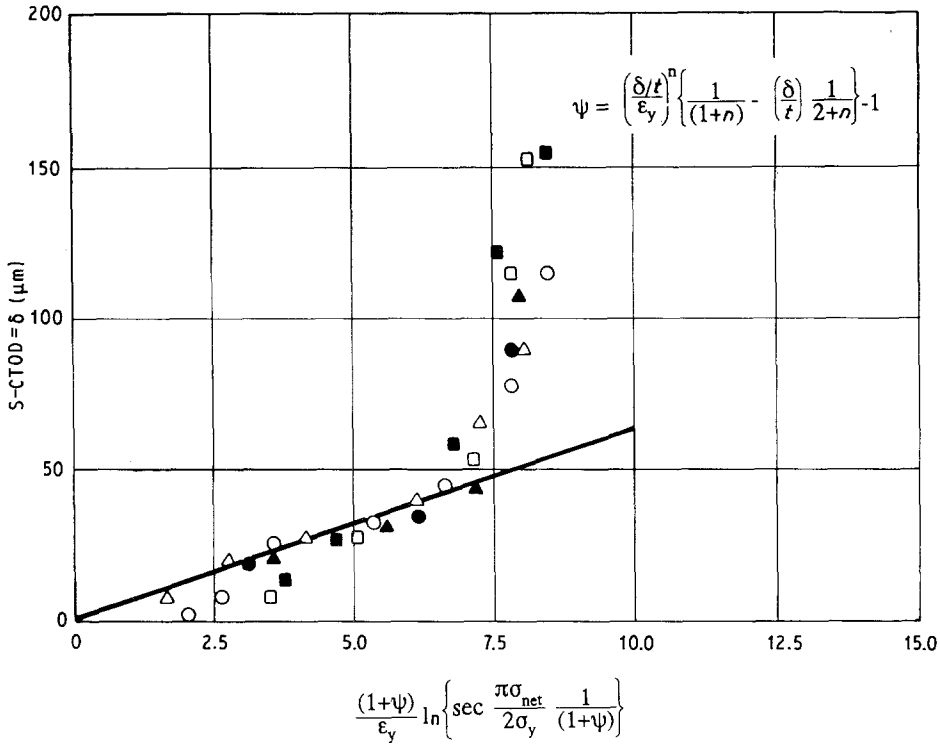

Figure 7 Variation of CTOD against an increase of loading according to the Isherwood–Williams model [37] for different thicknesses and α/w ratios. α/w: filled symbols = 0.1; open symbols = 0.5. d = △, 0.2; ○, 0.5; □, 1.2 mm.

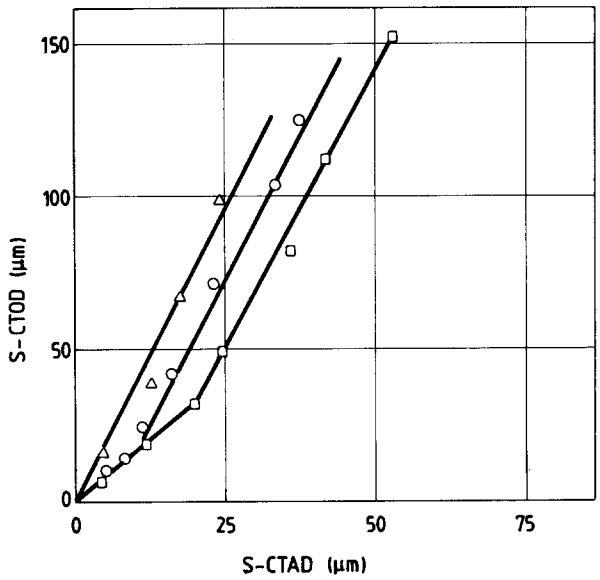

Figure 9 Variation of CTOD against CTAD for a series of SECT specimens of the same lateral constraint factor, $\alpha/w = 0.1$, and different thicknesses d: △, 0.2; ○, 0.7; □, 1.5 mm.

thick specimens ($d = 1.5$ mm) a longer first phase exists obeying Equation (1) than in thin specimens ($d = 0.7$ mm), whereas for very thin specimens ($d = 0.2$ mm) this first phase disappears totally.

Fig. 10 presents the variations of the critical S-CTODs, denoted here by δ_i, in terms of either the thickness, d, or the in-plane constraint factors α/w, as well as in terms of the angle β of the obliqueness of the crack or the angle φ of the rolling direction. For a certain thickness d_{cr} of the cracked plates, a maximum appears for δ_i. This critical value of thickness is $d_{cr} = 1.0$ mm. Fig. 10b presents the influence of the in-plane constraint factor α/w on δ_i, whereas in Fig. 10c the dependence of the critical S-CTOD on the obliqueness angle β of the crack, and therefore of the amount of mixed-mode loading, is indicated. Moreover in Fig. 10d the influence of the anisotropy of the material due to rolling and eventually to the recrystallization texture on the critical S-CTOD is presented.

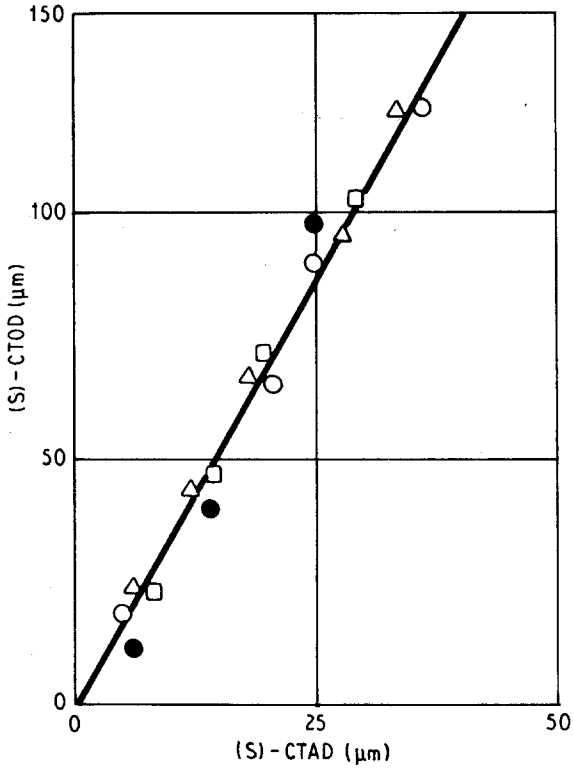

Figure 11 Variation of CTOD against CTAD for mixed-mode loadings of the copper plates, of the same thickness $d = 1.0$ mm and under angles of slant β = △, 30°, ○, 45° and □, 75°. ●, (S) DECT specimen.

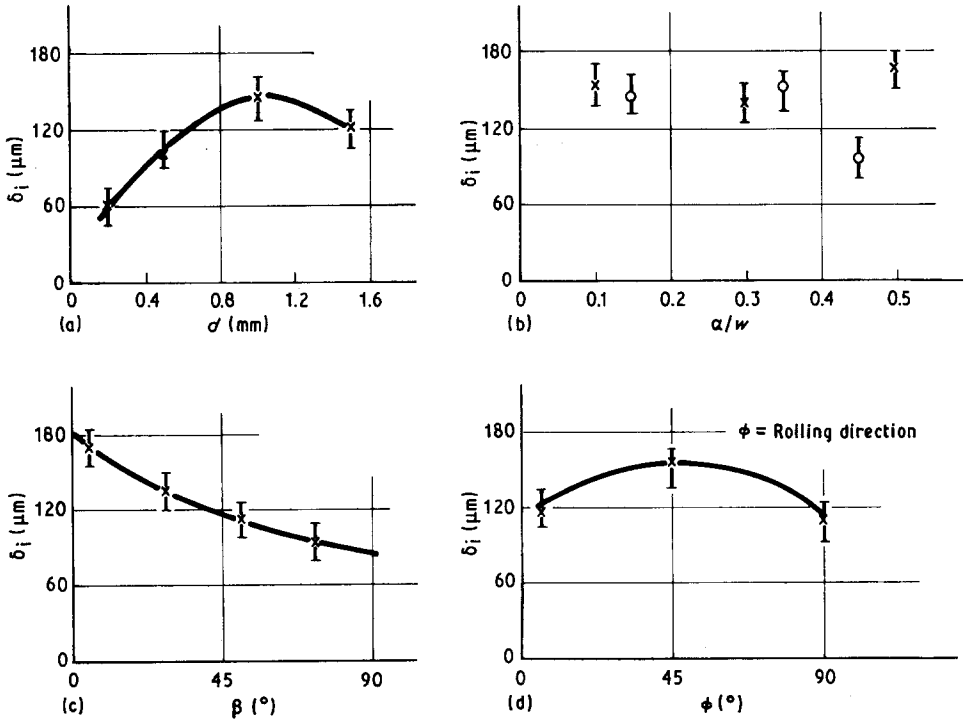

Figure 10 Variation of CTOD in terms (a) of the thickness d of specimens; (b) of the α/w ratio; (c) of the angle of slantness β; and (d) of the angle of orientation of rolling φ (c, d) $d = 1.0$ mm. (×) $d = 0.2$ mm, (○) $d = 0.7$ mm.

Finally, Fig. 11 presents the variation of the S-CTOD in terms of the S-CTAD for specimens of the same thickness $d = 1.0$ mm, whose cracks are oblique to different angles of obliqueness. It is evident from this figure that the influence of the angle β is insignificant for SECT and DECT specimens, indicating again that as the blunting of the crack evolves and the initiation of slow crack propagation approaches, the type of blunting is changing from a mixed-mode to a mode-I type of blunting.

4. Discussion

An extensive study of the blunting phenomena in polycarbonate has recently been undertaken [18]. As this material is highly polymeric, presenting a substantial viscoelastic region in its stress–strain diagram, followed by a plastic region with rather limited strain hardening, it is worthwhile to compare the results for blunting of this material with those for polycrystalline copper, whose stress–strain diagram presents a considerable strain hardening. Furthermore, copper is a crystalline material which presents many discontinuities in its texture at the boundaries of the grains, dislocations and other similar phenomena disrupting its continuity in the microscale.

An important difference between these two materials appears in the morphology of blunting, where for copper plates of the same thickness many more asperities on the surface around the blunted crack tip are apparent. The main reason for this phenomenon is probably the various destabilizing factors of metallurgical origin: grain boundaries, interstitials and others. For a certain thickness these factors cannot significantly influence the general aspect of blunting (i.e. its form, as round blunting, flat-front, and blunting with roots) but only some internal details.

This can be seen in Figs 2b and 3b where, for the same thickness of specimens, different morphologies of blunting appear, with many or few asperities. The general trend, however, is that with a reduction of the thickness of the specimen, the blunting pattern becomes smoother, without vertices, taking the form of an even, flat front terminating to the flanks of the crack under almost right angles. These observations are in disagreement with some theoretical studies defining probable forms of blunting for plane strain, for thick specimens [28, 29].

However, the most likely form of blunting under plane-stress conditions has been determined by the method of slip lines [20]. This form closely resembles the form of blunting appearing also in copper specimens, as shown in Figs 5 and 6.

The bright fields mentioned above are indications of a strong shear field of plastic flow, which appears clearly on both sides of blunting in Figs 3b and 4c, but also in front of the blunted crack tip in Figs 2c, 3a and 4c.

The phenomenon of surface roughening of metals is a general phenomenon known as the orange peel effect [40] which becomes more intense in the plastic flow zone around the crack tip [41]. It is well known that surface roughness increases as the slip planes of dislocation motion interact with the surface during plastic flow. Since slip planes of dislocation motion (gliding) are activated mainly from the shear fields, we may conclude that the bright fields appearing at the vicinity of the blunted crack are fields of localized plastic shear flow on both sides of the blunting, and also at some distance in front of the crack tip.

The localized shear flow covers exactly the zone of CTAD and therefore appears to be the cause of its evolution. This phenomenon is seen in Figs 2a and b, and 4a and b, where as long as the blunting is circular there is no shear flow, whereas as soon as an outflattened front begins to develop, the first step of CTAD is also apparent on both sides of the shear flow. The intense phenomenon of the average peel which appears clearly in Figs 2c and d is due to localized shear flow at some distance in front of the blunted surface, and is related to the initiation of necking by a delamination process of the external layers of the material, thus preparing the initiation of the crack propagation phase.

The whole phenomenon of the blunting formation through localized plastic flow in shear bands under plane-strain conditions has recently been studied [22]. The study of the mechanism of blunting in cracks under conditions of plane stress showed that this phenomenon is much more intense for cases of plane stress.

Fig. 2c and d as well Figs 4d and 6c clearly show the development of localized shear flow at some distance in front of the blunted crack tip. Thus just in front of the blunted crack tip, a dark field is interposed which is extended to a width approximately equal to the developed CTOD. The explanation for this is that the shearing delamination process in front of the crack is not extended up to the blunted front boundary, but stops some distance inside.

Even if the crack begins to propagate, as in Fig. 2c and d, the dark field is always there and it does not disappear by an extension of the bright field. This dark field always remains under conditions of reduced shear which do not develop delaminations. On the contrary, this restricted zone is under the influence of a triaxial state of stress which should be conserved and favoured by the large strain hardening of copper.

It may be concluded that in thin cracked plates in an advanced step of loading, where blunting phenomena have been largely evolved, a plastic zone under an intense triaxial mode of loading is developed approaching plane-stress conditions. The extent of this plastic zone is approximately equal to the respective CTOD developed in the blunted crack. Similar phenomena have been found previously for cracked plates made of polymers (polycarbonate) under plane-stress conditions [20].

Fig. 9 indicates that relations between S-CTOD and S-CTAD are of the form described by relations 1 or 2, which show how much each individual is closer to plane-stress or plane-strain conditions. The same phenomena are indicated qualitatively from the respective forms of blunting. Indeed, round blunting is connected with a prevalence of plane-strain conditions, especially along superficial layers, which later on tend to become

plane-stress conditions, and which activates a change in the form of blunting to an outflattened one with corners developed at its extremities.

Thus an initial constrained plastic flow at the crack tip is close to a plane strain with the ε_z strain through the thickness of the specimen tending to zero, and with a high hydrostatic tension also present. This hydrostatic tension is strengthened and conserved by the high degree of strain hardening presenting the copper specimens.

This state of loading of the plate may sometimes be so strong that it can maintain for a short period an intense state of plane strain, even on the external layers of the plate. However, this state is metastable and may be changed into a plane-stress due to the destabilization effect of asperities, as they are impurities, grain boundaries, interstitials etc. This phenomenon appears in Fig. 1, where the upper surface of the copper specimen presents a round blunting, whereas the lower surface is rather destabilized, and tends to a form of plane-stress blunting with an initiation of outflattening.

Thus an antagonism between two opposing phenomena appears to take place continuously as the loading progresses and blunting is evolved between the strain-hardening effect and the effect of metallurgical destabilizers, where specimens of the same thickness (presenting the same lateral constraint factor) may develop either of these extreme types of blunting.

In tests with polycarbonate specimens [18, 21] with the same thickness as those with copper, the round blunting mode did not appear at all, because of the complete lack of strain hardening of PC. Thus, the evolution of a triaxial state of stress in front of the blunted crack did not favour the development of such a type of blunting. Finally, it appears that the strain-hardening effect is stronger than any destabilization effect.

The change of the lateral constraint factor also significantly influences the critical CTOD (δ_i^{cr}). Fig. 10a indicates that δ_i^{cr} becomes a maximum for a certain thickness, and then diminishes both ways. The dependence of the critical value CTOD in terms of the thickness follows the same trend as the trend followed by other fracture parameters, as it is the K_I factor [15] and the evolution of plastic zone [42]. Therefore some kind of interrelation exists between these three fracture parameters.

The constrained plastic flow may influence the evolution of blunting. Thus the variation of the in-plane constraint factor because of the change in crack geometry from the SECT- to DECT-type of specimens influences the evolution of blunting. This is indicated in Fig. 8, where a strong plastic constraint developed in DECT specimens creates a larger time interval of dominance of the specimen surface under conditions of plane strain than with SECT-specimens.

The change of the ratio α/w in SECT specimens does not significantly change the mode of evolution of blunting. However, this remark cannot be interrelated quantitatively with the results with PC [18], as in PC there is also no connection between α/w and the mode of evolution of blunting, but in this material the phase of round blunting is almost completely missing. Indeed, round blunting in PC was expressed through Equation 2, whereas in copper the same phenomenon is expressed through Equation 1.

Thus while Equation 1 constitutes a sure criterion for any amount of deviation from strictly plane-strain conditions at the region of the crack tip, any eventual discrepancy from the results of the modified Dugdale model, which was applied in Fig. 7, may indicate a respective deviation from the ideal plane-stress conditions of loading. Fig. 7 clearly indicates a general trend that thin specimens correspond better than the thick specimens. Another result derived from this experimental study is that the modified Dugdale model does not exactly describe the blunting behaviour even for thin specimens, although it constitutes one of the best criteria, since it also takes into account the influence of the distribution of yield strength around the crack-tip area and, simultaneously, it also considers the amount of strain hardening of the material.

Fig. 11 presents the classical single-edge mixed-mode loading of a cracked plate and indicates that this does not influence the evolution of blunting, where for larger angles of slant of the crack the initial phase of the round blunting progressively disappears. The same phenomenon also appears for the mixed-mode geometry with the DECT specimens, where two skew cracks exist in the specimen. Both types of mixed-mode loading reduce the critical CTOD (δ_i^{cr}) as is evident in Fig. 10b. Similarly, the anisotropy of the material indicated in Fig. 10d does not significantly influence the critical CTOD, since only a small monotonic decrease of CTOD is seen with increasing anisotropy. The study of blunting evolution in DECT specimens was carried out according to ASTM standards [33] where the direction of plate rolling was parallel to the straight line connecting the tips of the two staggered cracks.

The common characteristic of the geometry for the two types of specimen (SECT and DECT) is the elimination of round blunting as the intense shear mode of deformation, K_{II}, represses the formation of round surface blunting, which necessitates a strong plane-strain deformation field. For this situation it is valid that $\varepsilon_z \approx 0$, and because of the plastic incompressibility state around the crack tip it is valid that $\varepsilon_x \approx -\varepsilon_y$ which results in a contraction deformation along the x–y plane, creating the type of blunting indicated in Fig. 7.

Simultaneously, a z-contraction deformation field develops through the thickness of the specimen, having a relaxation effect along this direction, which tends to a three-dimensional state of stress and strain approaching plane-stress conditions. This results in a smaller xy-contraction deformation creating a smaller CTAD.

As mentioned above, for the same CTOD we have smaller CTAD for polycarbonate [21] than for copper for intense plane-stress conditions, due to the large elastic compressibility of PC, a fact which reduces the CTAD in this material whereas in copper the larger CTAD is due to severe localized shear flows in front of the crack.

5. Conclusions

The study of evolution of the phases of blunting in copper specimens under mode-I and mixed-mode conditions, through direct observation and measurement by SEM, gave interesting results. It was possible to measure directly the parameters of CTOD and CTAD *in situ* during the evolution of phases of blunting.

Using theoretical models as measures of comparison, we succeeded in establishing a clear picture of the evolution of blunting and the influence exerted on it by the geometry of the specimens and the loading mode. Thus for mode I we can conclude that reduction of the specimen thickness tends to smooth the form of blunting, which from a form of an outflattened front containing roots with several vertices, becomes smooth with a flattened front.

The variation in thickness (and therefore the lateral constraint factor) results in the appearance of a maximum on the critical CTOD, which tends to stabilize itself to a limit for large thicknesses corresponding to plane-strain conditions. This factor is drastically reduced for thin specimens under dominating plane-stress conditions. The blunting under dominating plane-stress conditions is mainly due to a localized shear-flow field developed along the flanks of the crack.

For relatively thick specimens, the blunting is developed in two phases: firstly round blunting, corresponding to plane-strain conditions, then the flat type of blunting evolves, indicating a progressive development of conditions of plane stress. The variation of the in-plane constraint factor influences blunting during the transition from SECT to DECT geometry.

Experiments do not satisfactorily confirm the modified Dugdale model, as even very thin specimens present discrepancies from this model.

The typical simple mixed-mode and double staggered-crack model do not differ significantly in their influence on blunting evolution. Both models tend to reduce the critical CTOD and to eliminate the initial round type of blunting, developing from the beginning the asymmetrical flat blunting which, after its initial appearance, is dominated by a typical mode-I type of blunting even for mixed-mode loading.

The main factors influencing blunting are the amount of strain hardening and the eventual development of significant elastic compressibility in front of the crack. The difference in these two factors between copper and polycarbonate explains the differences in the blunting phenomena between these two typical materials (metals and polymers).

Acknowledgement

The authors are indebted to Mrs Anny Zografaki, secretary of the first author, for help in typing the manuscript.

References

1. A. A. WELLS, in "Proceedings of the Crack Propagation Symposium", Vol. 1 (College of Aeronautics, Cranfield, UK, 1961) Paper B4, p. 210.
2. C. G. CHIPPERFIELD, *Int. J. Fracture* **12** (1976) 873.
3. J. D. HARRISON, M. G. DAWES, G. L. ARCHER and M. S. KAMATH, ASTM-STP **668**, (American Society for Testing and Materials, Philadelphia, 1979) p. 606.
4. WEI-DI CAO and XIA-PING LU, *Int. J. Fracture* **25** (1984) 33.
5. M. G. DAWES, ASTM-STP **668**, (American Society for Testing and Materials, Philadelphia, 1976) p. 115.
6. P. S. THEOCARIS, *J. Strain Anal.* **9** (1974) 197.
7. W. N. SHARPE, Jr. and A. F. GRAND Jr., ASTM-STP **590** (American Society for Testing and Materials, Philadelphia, 1976) p. 302.
8. T. SHOJI, *Metal Sci.* **10** (5) (1976) 165.
9. T. SHOJI, H. TAKAHASHI and M. SIZUKI, *ibid.* **12** (12) (1978) 579.
10. J. N. ROBINSON, *Int. J. Fract.* **12** (1976) 723.
11. C. M. GILMORE, V. POVENZANO and F. A. SMIDT Jr., *Metal Sci.* **17** (1983) 177.
12. O. KOLEDNIK and H. P. STUWE, *Engng Fract. Mech.* **21** (1985) 145.
13. K. KASHIWAYA and T. YANUKI, *ibid.* **7** (1975) 551.
14. J. O. VOSIKOVSKY, *Int. J. Fract.* **10** (1974) 147.
15. D. BROECK, *Engng Fract. Mech.* **6** (1975) 121.
16. C. F. SHIH, *J. Mech. Phys. Solids* **29** (1981) 305.
17. M. OBATA and H. SHIMIDA, in "Proceedings of the Vth International Congress on Experimental Mechanics", Montreal 1984, (Society for Experimental Stress Analysis, 1985) p. 117.
18. P. S. THEOCARIS, N. V. KYTOPOULOS and C. N. STASSINAKIS, *J. Mater. Sci.* **24** (1989) 1121.
19. P. S. THEOCARIS and N. V. KYTOPOULOS, *ibid.* **25** (1990) 997.
20. P. S. THEOCARIS, *Engng Fract. Mech.* **31** (1988) 255.
21. P. S. THEOCARIS and N. V. KYTOPOULOS, *J. Mater. Sci.* **26** (1991) 3575.
22. T. H. LIN, *J. Mech. Phys. Solids* **12** (1964) 391.
23. A. NEEDLEMAN and V. TVERGAARD, ASTM-STP **803**, (American Society for Testing and Materials, Philadelphia, 1983) p. I-80.
24. J. A. ALIC and R. M. ASIMOV, *Engng Fract. Mech.* **6** (1974) 223.
25. J. S. KE and H. W. LIN, *ibid.* **5** (1973) 187.
26. J. E. HACK, K. S. CLAN and J. W. CARDINAL, *ibid.* **21** (1985) 75.
27. J. R. RICE and M. A. JOHNSON, in "Inelastic Behavior of Solids", edited by M. F. Kanninen (McGraw-Hill, New York, 1970) p. 641.
28. M. KAHL and K. REIFSNIDER, *Engng Fract. Mech.* **4** (1972) 653.
29. F. A. McCLINTOCK, in "Fracture – An advanced Treatise" III, (Academic, New York, 1971) p. 151.
30. J. R. RICE and M. A. JOHNSON, in "Inelastic Behavior of Solids", edited by M. F. Kanninen (McGraw-Hill, New York, 1970) p. 661.
31. J. C. HOWORD and A. A. WILLOUGHBY, In "Developments in Fracture Mechanics-2", edited by G. G. Chell (Applied Science, London, 1981) p. 66.
32. K. H. SCHWALBE, *Engng Fract. Mech.* **6** (1974) 415.
33. B. COTTERELL, E. LEC and Y. W. MAI, *Int. J. Fract.* **20** (1982) 243.
34. P. S. THEOCARIS and E. E. GDOUTOS, *ibid.* **10** (1974) 549.
35. G. E. TARDIFF, B. A. KUHN and L. A. HELDT, ASTM-STP **590**, (American Society for Testing and Materials, Philadelphia, Pennsylvania, 1976) p. 115.
36. J. C. NEWMAN Jr., *Engng Fract. Mech.* **1** (1968) 137.
37. D. P. ISHERWOOD and J. G. WILLIAMS, *ibid.* **2** (1970) 19.
38. J. C. HOWARD and N. R. OTTER, *J. Mech. Phys. Solids* **23** (1975) 139.
39. D. N. FENNER, *Int. J. Fract.* **10** (1974) 71.
40. C. E. HARRIS and D. H. MORRIS, in "Proceedings of the Vth International Congress on Experimental Mechanics", Montreal 1984 (Society for Experimental Stress Analysis, 1985) p. 743.

41. "Metals Handbook", Vol. **8**, edited by I. Lyman (American Society for Metals, Ohio, USA, 1973) p. 212.
42. J. H. UNDERWOOD, J. L. SWEDLOW and D. P. KENDALL, *Engng Fract. Mech.* **2** (1971) 183.
43. F. A. McCLINTOCK and A. S. ARGON, in "Mechanical Behavior of Materials" (Addison-Wesley, Reading, Massachusetts, 1966) p. 276.

Received 5 March
and accepted 1 July 1991